To cite this article: ZI H, LI Y G, HU M, et al. Flexural wave bandgap and isolation characteristics of vibration and sound in periodic sandwich plates [J/OL]. Chinese Journal of Ship Research, 2023, 18(2). http://www.ship-research.com/en/article/doi/10.19693/j.issn.1673-3185.02462.

DOI: 10.19693/j.issn.1673-3185. 02462

Flexural wave bandgap and isolation characteristics of vibration and sound in periodic sandwich plates

ZI Huan[1,2], *LI Yinggang*[1,2,3], *HU Mi*[2,1], *ZHU Fengna*[*1,2], *ZHU Ling*[1,2,3]

1 Key Laboratory of High Performance Ship Technology of the Ministry of Education, Wuhan University of Technology, Wuhan 430063, China

2 School of Naval Architecture, Ocean and Energy Power Engineering, Wuhan University of Technology, Wuhan 430063, China

3 Sanya Science and Education Innovation Park, Wuhan University of Technology, Sanya 572025, China

Abstract: [**Objective**] This paper aims to study the elastic wave propagation characteristics and vibration and noise reduction mechanisms of periodic ship sandwich plates. [**Method**] To this end, the dispersion relation and flexural wave bandgap characteristics of lightweight sandwich plates are numerically investigated using the finite element method in combination with the Bloch theorem. The flexural vibration and sound transmission properties are analyzed to study vibration and sound reduction, and experimental validation is further conducted to verify the numerical results. [**Results**] Lightweight sandwich plates can yield flexural wave bandgaps in a specific frequency range due to the Bragg scattering effect, resulting in flexural vibration isolation and sound insulation. [**Conclusion**] Flexural wave bandgaps can be effectively tuned by geometrical parameters, and this technology can potentially be applied in the vibration and sound control of ship structures.

Key words: periodic sandwich plates; flexible wave bandgap; Bragg scattering; vibration and sound reduction

CLC number: U663.7; U668.5

0 Introduction

With the continuous advancement of the maritime power strategy and the vigorous development of maritime traffic, the problems of ship structural vibration and underwater acoustic radiation have become increasingly prominent. The excitation source of ship vibration noise has the characteristics of large power and wide spectrum distribution. It mainly transmits vibration in the form of low-frequency flexural waves in the hull plate and radiates noise to the air and water, which seriously affects the comfort of ships and the concealment of vessels. Therefore, the vibration and noise reduction technology of ship structures has always been a hot issue concerned by scholars in China and abroad [1-6].

Phononic crystal is a new type of periodic structure with elastic wave bandgaps, which has a wide range of potential applications in the fields of ship vibration and noise reduction and acoustic stealth [7-9]. Sun et al. [10] used the finite element method to calculate the energy band structure and frequency response of the periodically ribbed plate. They also analyzed its vibration bandgap characteristics and

Received: 2021－07－26 **Accepted**: 2022－02－09

Supported by: National Natural Science Foundation of China (11972269); Natural Science Foundation of Hainan Province (521MS068)

Authors: ZI Huan, female, born in 1996, master degree candidate. Research interests: ship vibration noise control. E-mail: 13437189654@163.com

LI Yinggang, male, born in 1988, Ph.D., associate professor. Research interest: ship vibration noise control. E-mail: liyinggang@whut.edu.cn

ZHU Fengna, female, born in 1988, master, experimenter. Research interest: ship structural vibration and impact protection. E-mail: zhufn2016@whut.edu.cn

***Corresponding author**: ZHU Fengna

the influence of geometric parameters on the bandgap. In combination with the experimental method, Li et al. [11] studied the vibration isolation mechanism of periodic hull plates using the finite element method. They discussed the application of the acoustic metamaterial design concept in vibration and noise reduction of ships and marine engineering equipment. For the vertical vibration excitation of a certain type of ship, Ruan et al. [12] designed a single-phase spiral phononic crystal according to the local resonance mode and studied the vibration isolation characteristics of acoustic metamaterials, which has spiral local resonance-plate type, under different boundary conditions and load conditions. Guo et al. [13] proposed a phononic crystal plate with an additional cylindrical vibrator for vibration noise control of ship equipment and structures. They found that the phononic crystal plate had good vibration and sound insulation effects in a specific frequency range.

With the development of large-scale, high-speed, and lightweight ships, sandwich structures with lightweight high strength, large bending stiffness, and good impact resistance have attracted the attention of ship industry personnel in various countries. Due to the characteristics of lightweight, high specific strength, and high specific stiffness, the low-frequency vibroacoustic performance of sandwich structures is usually not ideal. Therefore, some scholars have carried out acoustic design based on the generation mechanism of the bandgap characteristics and studied the bandgap characteristics of sandwich superstructures. Jiang et al. [14] attached the isotropic aluminum plate to the upper and lower sides of a one-dimensional phononic crystal and proved that this structure had bandgap characteristics. The larger the thickness of the core layer and the larger the proportion of soft rubber in the core layer, the more favorable it is for the opening of the low-frequency bandgap. Chen et al. [15-17] studied the propagation characteristics of elastic waves in sandwich structures with periodic core layers and embedded local resonators, and the core layer or sandwich plate was equivalent to a homogeneous structure. Experimental and numerical results showed that the structure can generate bandgaps in a certain frequency range, thereby suppressing elastic waves and vibration propagation. Li et al. [18] embedded a local resonator equivalent to a resonator in the core layer of the sandwich plate to study its acoustic characteristics, and it effectively improved the acoustic performance of the sandwich plate. Song et al. [19 - 21] studied the acoustic transmission, acoustic radiation, and vibration characteristics of the structure and the influence of boundary conditions on its vibroacoustic characteristics by periodically arranging the local resonators on the sandwich plate. The results showed that the application of local resonators can produce bandgaps in the sandwich plate, thereby effectively improving its vibroacoustic characteristics in a certain frequency range. In the above literature, the low-frequency bandgap of the sandwich structure has a strong dependence on the local resonator. The solid equivalent unit is used to model the sandwich microstructure, so that the dynamic response of the core layer' microstructure in the wave propagation is ignored, and the propagation law of the wave in the actual sandwich structure cannot be revealed. At the same time, the introduction of the local resonator harms the light weight of the structure. On the other hand, the bandgaps of existing sandwich structures and their acoustic metamaterials are in the middle and high-frequency bands above 1 kHz, and how to break through the low-frequency bandgap below 1 kHz is urgent to be solved for the needs of ship engineering.

In this paper, the finite element numerical simulation and experimental test are combined to study the dispersion relation and vibration and noise reduction characteristics of periodic lightweight sandwich plates and reveal the propagation law of flexural waves and the generation mechanism of low-frequency bandgaps, thereby promoting its application in the fields of ship vibration and noise reduction and acoustic stealth.

1 Physical model and calculation method

1.1 Physical model

In this paper, the installation stiffened plate of a ship transformer base was selected as the research object. As shown in Fig. 1(a), the installation plate is composed of skin, web, and elbow plate. The transformer is fixed on the base, and the plate is simply supported around. The thickness of the base elbow plate is 4 mm, and the geometric parameters of the stiffened plate are shown in Table 1, where the longitudinal spacing is 250 mm and the rib spacing is 300 mm. According to the principle of similarity theory, combined with the neutral axis height, section area, and section modulus of the transverse and longitudinal sections of the stiffened plate, the equivalent design of the lightweight sandwich plate was carried out, and the geometric sketch of the lightweight sandwich plate was obtained as shown in Fig. 1(b). The lightweight sandwich plate is composed of the upper and lower panels and the middle cross-grid core layer with 10 periods in the x direction and 5 periods in the y direction. According to the phononic crystal lattice theory, the primitive cell model of the lightweight sandwich plate is shown in Fig. 1(c). The lattice constant a = 100 mm, the panel thickness e = 0.9 mm, the core grid wall thickness b = 0.9 mm, and the core height H = 40 mm. The steel material was selected as the lightweight sandwich plate. The material parameters are defined as elastic modulus E = 200 GPa, Poisson's ratio ν = 0.3, and density ρ = 7 800 kg/m^3.

Under the same boundary conditions and loading conditions, the static analysis of the ship stiffened plate and the periodic sandwich plate was carried out. The loading method, material properties, and grid types are consistent, and the calculation results are shown in Fig. 2. It can be seen from the figure that the strength and stiffness of the equivalently designed ship sandwich plate are better than those of the stiffened plate. Compared with the traditional stiffened plate, the ship sandwich plate has the advantages of lightweight and high strength and can meet the mechanical requirements of ship structure.

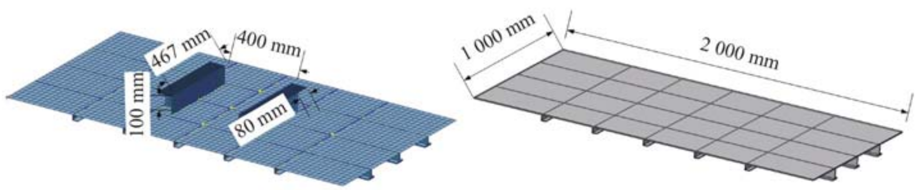

(a) Installation stiffened plate of a ship transformer base

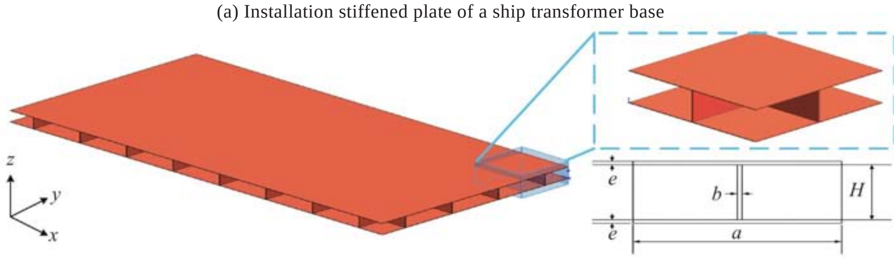

(b) Lightweight sandwich plate (c) Primitive cell model of the lightweight sandwich plate

Fig. 1 Schematic diagram of periodic lightweight sandwich plate

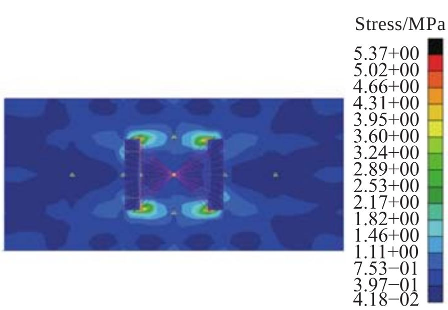

(a) Ship stiffened plate

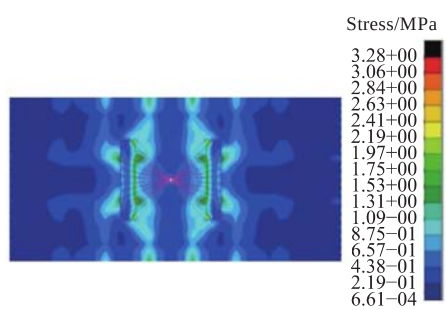

(b) Periodic sandwich plate

Fig. 2 Strength analysis of stiffened plate and periodic sandwich plate of ship

Table 1 Geometric parameters of stiffened plate

Parameter	Value
Panel length/mm	2 000
Panel width/mm	1 000
Panel thickness/mm	6
Longitudinal bone (T profile) specification/mm	TN 50 ×50 ×5 ×7
Rib (L profile) specification/mm	L 30 ×3

1.2 Calculation method

The finite element software COMSOL Multiphysics 5.4 was used to analyze the characteristic frequency of the lightweight sandwich plate, calculate the energy band structure, and use the shell element to model the sandwich plate. The type of the shell element is the tensor mixed interpolation plate and shell element (MITC plate and shell element), which is developed from the Mindin-Reissner plate and shell theory. The Mindin-Reissner plate and shell theory improves the assumption of straight normal in the Kirchhoff plate and shell theory. The normal perpendicular to the middle plane before deformation remains straight after deformation, and the displacement and rotation in the thickness direction of the plate are independent of each other. The flexural wave equation of the plate in the Mindlin-Reissner plate and shell theory is

$$-\rho h\frac{\partial^2 w}{\partial t^2}=\frac{\partial^2}{\partial x^2}\left[D\left(\frac{\partial^2 w}{\partial x^2}+\frac{\partial^2 w}{\partial y^2}\right)\right]+2\frac{\partial^2}{\partial x\partial y}\left[D\frac{\partial^2 w}{\partial x\partial y}\right]-\frac{\partial^2}{\partial t^2}\left(\frac{\partial}{\partial x}\left(\left(\frac{\kappa\rho}{G}+\rho J\right)\frac{\partial w}{\partial x}\right)+\frac{\partial}{\partial y}\left(\left(\frac{\kappa\rho}{G}+\rho J\right)\frac{\partial w}{\partial y}\right)\right)+\left(\frac{\kappa\rho}{G}J\right)\frac{\partial^4 w}{\partial t^4} \tag{1}$$

where w is the out-of-plane displacement; h is the plate thickness; D is the bending stiffness; G is the shear modulus; κ is the shear correction factor; J is the moment of inertia. Among them,

$$\begin{cases} G=\dfrac{E}{[2(1+\nu)]} \\ \kappa=20\dfrac{(1-\nu)}{(24+25\nu+\nu^2)} \\ J=\dfrac{h^3}{12} \end{cases} \tag{2}$$

According to the finite element principle, the elastic wave equation in the primitive cell can be discretized into a generalized eigenvalue equation:

$$\left(\boldsymbol{K}-\omega^2\boldsymbol{M}\right)\boldsymbol{u}=\boldsymbol{F} \tag{3}$$

where $\boldsymbol{K}$ is the stiffness matrix; $\boldsymbol{M}$ is the mass matrix; $\boldsymbol{u}$ is the eigenvector matrix; $\boldsymbol{F}$ is the external force matrix; ω is the sound wave frequency.

Based on the energy band theory in solid lattice and Bloch theorem, the lattice of lightweight sandwich plates has periodicity and point group symmetry, and its eigenfield has the form of the Bloch function. The eigenfunction of the wave equation is a plane wave periodically amplitude-modulated according to the positive lattice:

$$\boldsymbol{u}(\boldsymbol{r}+\boldsymbol{a})=\boldsymbol{u}(\boldsymbol{r})\mathrm{e}^{\mathrm{i}(\boldsymbol{k}_r\boldsymbol{a})} \tag{4}$$

where $\boldsymbol{k}_r$ is the wave vector, and its value is limited to the first Brillouin zone; $\boldsymbol{r}$ is the spatial position vector; $\boldsymbol{a}$ is the lattice constant vector.

According to the periodic boundary conditions, Floquet periodic boundary conditions are added in the x and y directions respectively to indicate that the lightweight sandwich plate is periodic in the x and y directions. The wave propagation of the lightweight sandwich plate is transformed into the following eigenvalue problem for solving:

$$\left|\boldsymbol{K}'(k_x,k_y)-\omega^2\boldsymbol{M}'(k_x,k_y)\right|=0 \tag{5}$$

where k_x and k_y are the wave vector components in the x and y directions, respectively.

$$\boldsymbol{K}'=\boldsymbol{R}^{\mathrm{H}}(k_x,k_y)\boldsymbol{K}\boldsymbol{R}(k_x,k_y),\boldsymbol{M}'=\boldsymbol{R}^{\mathrm{H}}(k_x,k_y)\boldsymbol{M}\boldsymbol{R}(k_x,k_y) \tag{6}$$

$$\boldsymbol{R}=\begin{bmatrix} 1 & 0 & 0 & 0 & 0 & 0 & 0 & 0 & 0 \\ 0 & \mathrm{e}^{-\mathrm{i}k_y a_y} & \mathrm{e}^{-\mathrm{i}k_x a_x-\mathrm{i}k_y a_y} & 1 & \mathrm{e}^{-\mathrm{i}k_x a_x} & 0 & 0 & 0 & 0 \\ 0 & 0 & 0 & 0 & 0 & 1 & \mathrm{e}^{-\mathrm{i}k_x a_x} & 0 & 0 \\ 0 & 0 & 0 & 0 & 0 & 0 & 0 & \mathrm{e}^{-\mathrm{i}k_y a_y} & 1 \end{bmatrix}^{\mathrm{T}} \tag{7}$$

where $\boldsymbol{R}^{\mathrm{H}}$ is the conjugate matrix of $\boldsymbol{R}$; a_x and a_y are the lattice constants in the x and y directions, respectively. If a set of Bloch wave vectors (k_x, k_y), are given, then a set of eigenvalues and eigenvectors can be obtained.

For finite periodic structures, the transmission characteristics are usually described by the frequency response function between the structural excitation end and the response end. For the structural vibration transmission characteristics in the solid physical field, they can be indicated with vibration transmissibility:

$$T_{\mathrm{r}}=20\lg(a_{\mathrm{out}}/a_{\mathrm{in}}) \tag{8}$$

where a_{in} is the acceleration excitation at input end; a_{out} is the acceleration response at output end.

When describing the transmission characteristics of sound waves, we usually use decibels as a measure, and the sound reduction expressed in decibels is called the sound reduction index (S_{TL}):

$$S_{\mathrm{TL}}=10\lg(1/t_{\mathrm{I}})=20\lg(p_{\mathrm{ia}}/p_{\mathrm{ta}}) \tag{9}$$

where t_{I} is the transmission coefficient of sound intensity; p_{ia} is incident sound pressure; p_{ta} is transmitted sound pressure.

2 Flexural wave bandgap and vibration and sound reduction characteristics in lightweight sandwich plates

According to the above theoretical basis, the energy band structure and transmission characteristics of the lightweight sandwich plate are calculated by the finite element method. Fig. 3(a) is the calculation model of the dispersion relation of the primitive cell for the lightweight sandwich plate. Combined with the Bloch theorem and solid lattice theory, the Floquet periodic boundary conditions are added in the x and y directions when calculating the dispersion relation of the lightweight sandwich plate, so as to indicate that the ship sandwich plate is periodic in the x and y directions. The free triangular gird is used for grid division on the thin shell structure. The number of girds is 6 386, and the maximum size of the gird is 3.5 mm. According to the solid lattice theory and Bloch theorem, due to the translational symmetry and point group symmetry of the crystal, the characteristic frequency of the primitive cell in all directions can be obtained when the wave vector is scanned along the boundary of the first irreducible Brillouin zone. Taking the wave vector direction as the abscissa and the characteristic frequency as the ordinate, the energy band structure of the lightweight sandwich plate can be obtained. Fig. 3(b) is the calculation model of vibration transmission characteristics of lightweight sandwich plates with finite periodicity. If the unit acceleration excitation a_{in} along the z direction is applied at one side of the calculation model and the acceleration response is detected on the opposite side, the vibration transmission characteristic curve can be obtained by calculating the vibration transmissibility in the range of 1−1200 Hz according to Eq. (6).

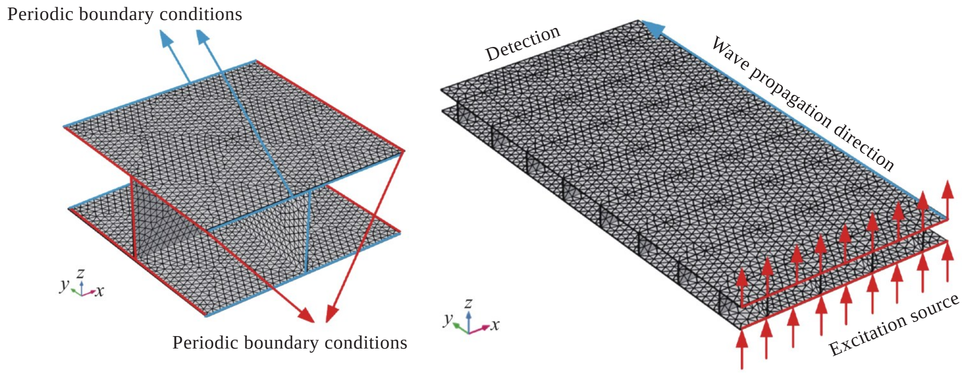

(a) Primitive cell model (b) Lightweight sandwich plate with finite periodicty

Fig. 3 Finite element calculation model

The energy band structure and transmission characteristics of the lightweight sandwich plate were calculated by 3D solid mechanics-shell physical field, as shown in Fig. 4. It can be seen from the figure that there are five energy bands in the frequency range of 0−1 200 Hz, three of which start from point Γ and include the basic plate wave modes, namely flexural wave (antisymmetric Lamb wave A_0 mode), horizontal shear wave (S_{H0} mode), and longitudinal wave (symmetric Lamb wave S_0 mode). The remaining energy bands are the coupling results of the high-order forms of the basic plate waves. Due to the periodic Bragg scattering effect of the lightweight sandwich plate, the flexural wave bandgaps appear in the frequency range of 699−971 Hz, and the flexural vibration of the sandwich plate in the bandgap frequency range is effectively suppressed.

To further explore the engineering application of ship periodic sandwich plates in vibration and noise

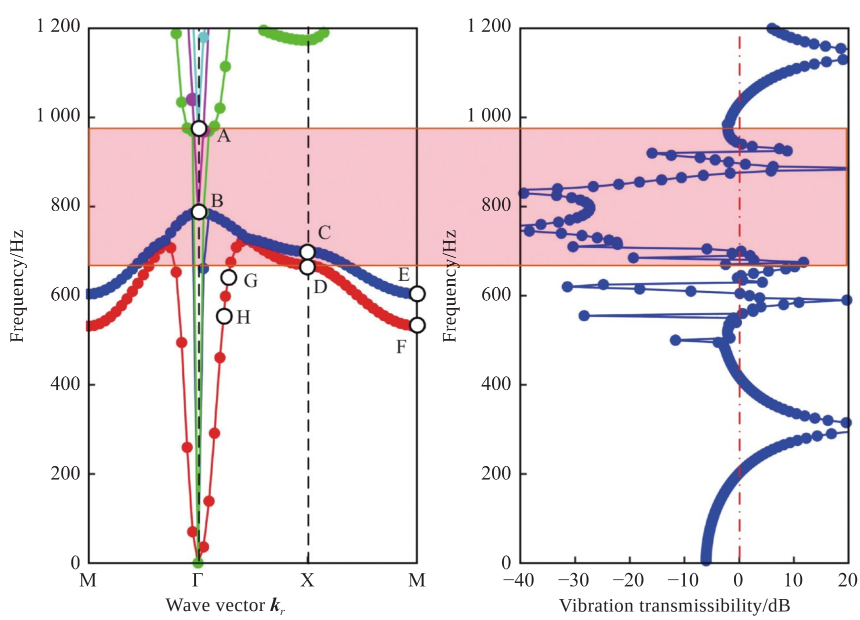

(a) Enerygy band structure (b) Transmission characteristics

Fig. 4 Flexural wave bandgap and vibration isolation characteristics of lightweight sandwich plate

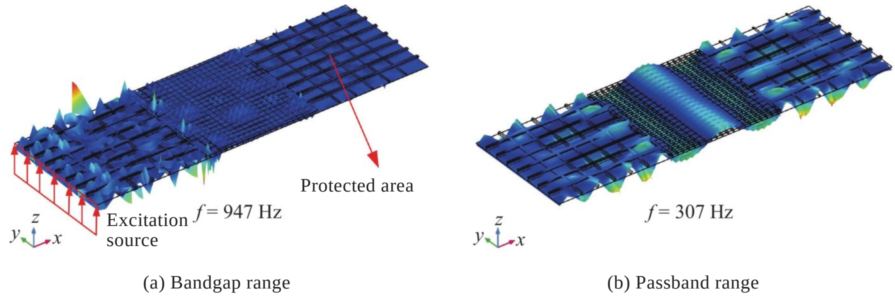

Fig. 5 Flexural vibration transmission and attenuation characteristics of lightweight sandwich plate

reduction of ship power systems, taking the low-frequency excitation source of a ship transformer as the control object, the ship periodic sandwich plate was arranged between the power source and the protected area, and the acceleration excitation was applied to the power source to simulate the low-frequency excitation of the transformer to calculate the vibration transmissibility respectively. Figs. 5(a) and (b) show the effect of vibration transmission characteristics of finite periodic lightweight sandwich plates in the bandgap frequency range (f = 947 Hz) and the passband frequency range (f = 307 Hz), respectively. It can be seen from the figure that when the excitation frequency is in the bandgap, the flexural vibration excitation source of the ship power system is limited to the first few periods of the finite periodic lightweight sandwich plate. The lightweight sandwich plate has a significant attenuation effect on the flexural vibration in the bandgap frequency range, which can play an effective role in vibration isolation.

To analyze the sound insulation characteristics of the lightweight sandwich plate, the acoustic-solid coupling method in Ref. [22] was referred to calculate the sound reduction index of the lightweight sandwich plate. The lightweight sandwich plate was placed in the pressure acoustic physical field; the air density was 1.225 kg/m^3, and the sound velocity in the air was set to 343 m/s. The upper and lower boundaries of the air layer are boundary conditions of plane wave radiation to simulate the infinite non-reflective sound field. The gird size of the finite element calculation model of the sound reduction index is less than 1/6 of the sound wavelength in the medium, which meets the requirements of calculation accuracy. A plane-wave acoustic pressure load with an amplitude of 1 Pa was applied at the lower boundary of the air layer, and the acoustic pressure values of the incident sound field and the transmitted sound field were measured. Based on the three-microphone method and the calculation formula of the sound reduction index, the curve for sound reduction index of the lightweight sandwich plate can be obtained. According to the sound insulation theory and mass law of infinite homogeneous wall plates, the sound insulation characteristic curve can be divided into the stiffness control area, modal resonance area, mass control area, and coincidence effect area. The average sound reduction index of homogenous single-layer plates is

$$S_{\mathrm{TL}} = 10\lg\left(\frac{\omega M_2}{2R_1}\right)^2 = -42 + 20\lg f + 20\lg M_2 \quad (10)$$

where R_1 represents the characteristic impedance of the medium; M_2 represents the mass per unit area.

As the surface density of the lightweight sandwich plate was 14.04 kg/m^2, the comparison results of the sound reduction index of the lightweight sandwich plate calculated according to the mass law are shown in Fig. 6. It can be seen from the figure that the sound reduction index curve of the lightweight sandwich plate is basically consistent with the calculation results of the mass law in the low-frequency band. However, the sound reduction index curve of the lightweight sandwich plate has a peak frequency band of sound insulation near 821 Hz, and its sound pressure field and structural vibration modes are shown in Fig. 6(b). When the frequency of incident sound wave is 821 Hz, the cloud diagram of vibration displacement on the side plate of the incident sound source is similar to the first-order flexural wave (antisymmetric Lamb wave) mode of the structure. The average vibration velocity of the side plate surface of the transmitted sound source is close to 0, and the incident sound wave energy is largely reflected, resulting in a peak value of sound reduction index. The peak frequency range of the sound reduction index is basically consistent with the frequency range of the flexural wave bandgap, and the sound reduction index is much higher than that of the lightweight sandwich plate calculated based on the mass law, indicating that the lightweight sandwich plate has a good sound insulation effect in the frequency range of the

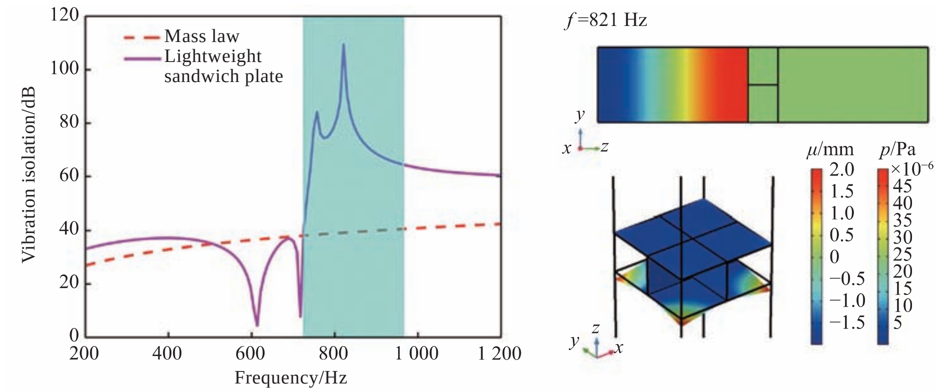

(a) Comparison of actual sound insulation and mass law (b) Sound pressure field and structural vibration mode

Fig.6 Sound insulation characteristics of lightweight sandwich plate

flexural wave bandgap, which can break through the limitation of the sound insulation mass law to a certain extent.

To further reveal the flexural wave bandgap and vibration and noise reduction mechanism of ship periodic sandwich plates, we analyzed the intrinsic mode of the single cell. Figs. 7(a)−7(c) show the propagation modes of asymmetric Lamb wave. Among them, the four angles of the primitive cell of the ship sandwich plate (Fig. 7(a)) vibrate in the same direction along the *z*-axis at the same time. The diagonals of the primitive cell of the ship sandwich plate (Fig. 7(b)) vibrate in the same direction along the *z*-axis at the same time. As shown in Fig. 7(c), the adjacent corners of the primitive cell of the ship sandwich plate on the *y*-axis vibrate in the same direction along the *z*-axis at the same time. The energy band shown in Figs. 7(a)−7(c) belong to the first-order flexural wave one, which is the basic propagation mode of asymmetric Lamb waves. The four-corner phase difference of wave propagation between the three is caused by the change in the wave vector direction. Through the modal analysis method [23], it can be seen that the flexural wave bandgap of the ship sandwich plate is between point A and point C. Therefore, the reason for the flexural wave bandgap of the ship sandwich plate is the truncation of the first-order flexural wave bandgap caused by the wave mode conversion.

The propagation mode shown in Figs. 7(d)−7(f) belongs to the one of the symmetric Lamb wave. As shown in Fig. 7(d), the upper and lower panels of the four corners of the primitive cell of the ship sandwich plate vibrate along the opposite direction of the *z*-axis at the same time, resulting in the simultaneous expansion and compression of each grid of the ship sandwich plate. As shown in Fig. 7(e), the upper and lower panels of the diagonal of the primi-

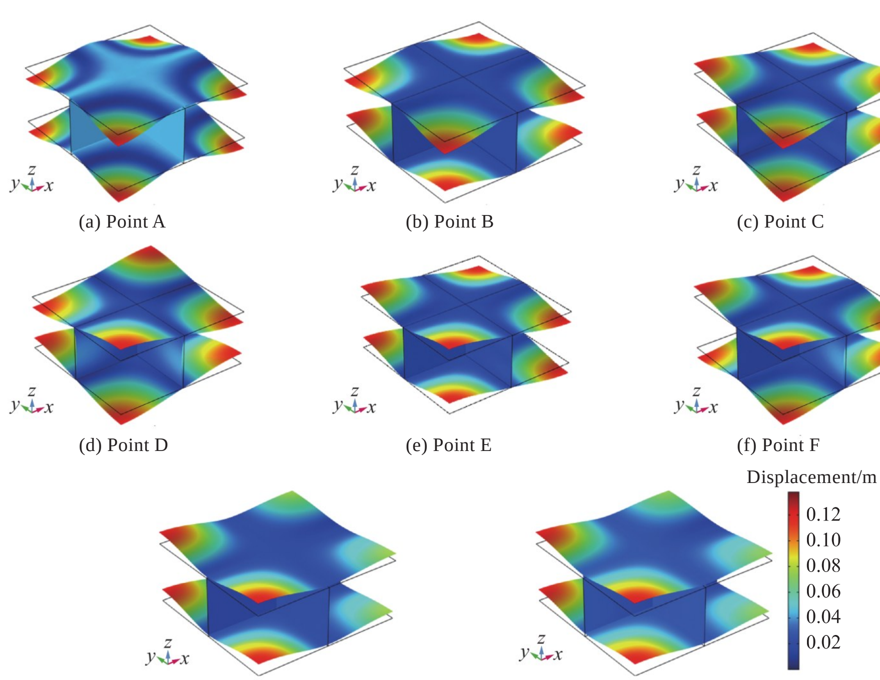

(a) Point A (b) Point B (c) Point C

(d) Point D (e) Point E (f) Point F

(g) Point G (h) Point H

Fig. 7 Eigenmodes of the primitive cell of periodic lightweight sandwich plate tive cell of the ship sandwich plate vibrate in the opposite direction along the z-axis. In Fig. 7(f), the upper and lower panels of the adjacent corners of the primitive cell of the ship sandwich plate on the y-axis is simultaneously vibrate in the opposite direction of the z-axis. The energy band shown in Figs. 7 (d)−7(f) belongs to the one of the first-order symmetric Lamb wave, which is the dominant eigenmode of the symmetric Lamb wave propagation mode, and it is not easy for the flexural wave to excite the structural vibration response under this mode.

It can be seen from Fig. 7(g) and 7(h) that the eigenmodes corresponding to point G and point H belong to the asymmetric Lamb wave propagation mode. Therefore, it is easy for the flexural vibration to excite the structural vibration response here.

From the analysis of the eigenmodes of the primitive cell of the ship sandwich plate, it can be seen that the reason for the flexural wave bandgap of the periodic ship sandwich plate is that the flexural wave is reflected back and forth at each periodic boundary under the Bragg scattering modulation of the lattice, and the forward wave and the reverse wave will destructively interfere so that the flexural wave of certain frequencies has no corresponding flexural vibration mode in the periodic structure, which ultimately leads to the flexural wave bandgap.

To verify the simulation results, we tested the vibration transmission characteristics of the lightweight sandwich plate. The size of the sandwich plate is the same as that set in the simulation. The instruments used in the experiment include the M+P test system, power amplifier, computer for installing control and analysis software, B&K 4507 accelerometer, and vibrator, as shown in Fig. 8. The sandwich plate is suspended in the air by a flexible rope; the excitation rod of the vibrator is installed on one side of the lightweight sandwich plate, and an accelerometer is installed on this side to measure the vibration acceleration at the input end. Another accelerometer is installed on the output end to measure the output vibration acceleration. The data collected by the accelerometers are transmitted to the M+P test system for conversion, and the acceleration responses at the input end and the output end are calculated using the vibration transmissibility formula, thereby obtaining the vibration transmission characteristics.

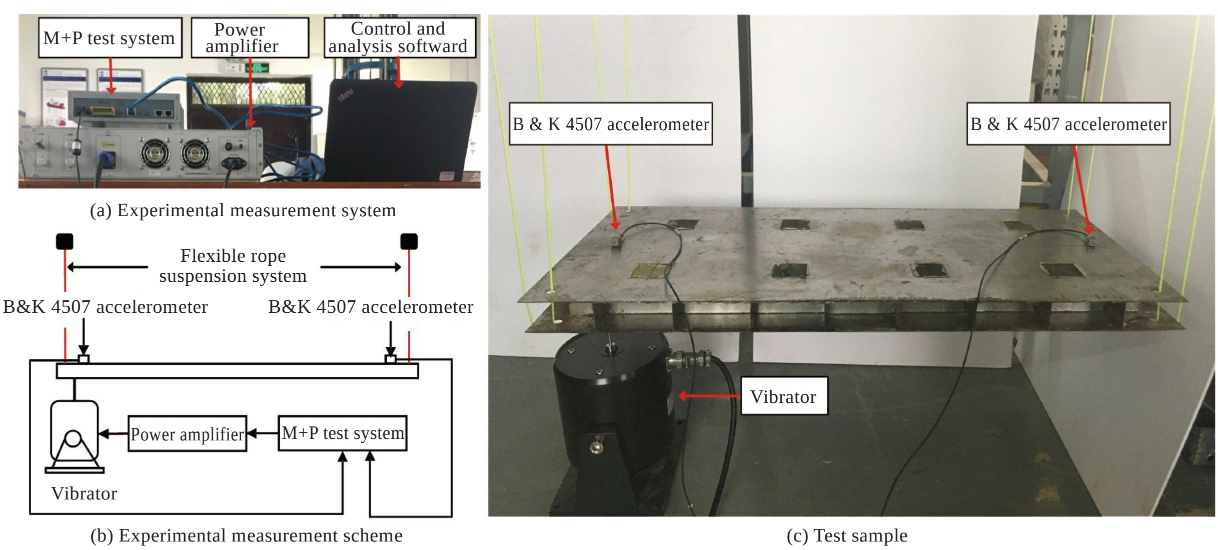

Fig. 8 Test sample and experimental measurement setup

Using the above experimental test platform, three experiments were repeated, and the frequency response function of the lightweight sandwich plate sample with finite periodicity was obtained, as shown in Fig. 9. It can be seen from the figure that there is a significant attenuation area in the frequency range of 580−949 Hz for the flexural vibration transmission characteristics of ship periodic lightweight sandwich plates. The frequency range of flexural vibration attenuation is in good agreement with that of the flexural wave bandgap of lightweight sandwich plates, which verifies the reliability of the numerical calculation method for flexural wave bandgaps and vibration reduction characteristics of lightweight sandwich plates. At the same time, it is found that the lower limit of the flexural wave bandgap obtained by the experiment is lower than that obtained by the simulation, and the bandwidth of the flexural wave obtained by the experiment is wider than that obtained by the simulation.

The main reasons for the difference between the experimental test results and the simulation results may be as follows: 1) in the actual test sample, the connection of the upper and lower panels with the core layer is adhesive, which leads to the decrease in the overall stiffness of the sandwich plate, so the initial frequency of the bandgap moves down; 2) the simulation does not consider the influence of material damping, and in the actual test sample, the existence of structural damping broadens the bandwidth and attenuates the resonance peak.

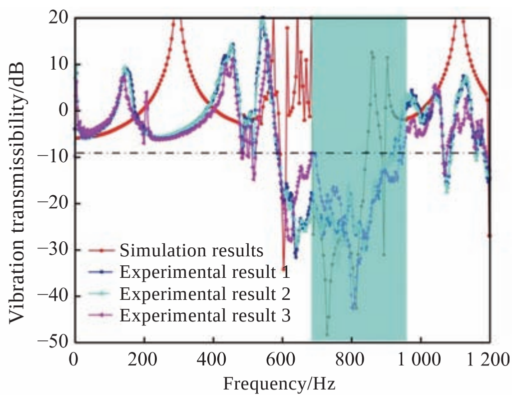

Fig. 9 Experimental validation of frequency spectra

3 Influence of structural parameters on flexural wave bandgaps

According to the analysis on the generation mechanism for the flexural wave bandgap of the periodic sandwich plate in ship, it can be seen that the starting frequency and cutoff frequency of the flexural wave bandgap of the lightweight sandwich plate are related to its energy band distribution. It is found that the change of geometric parameters will lead to a series of regular changes in the distribution of energy band structure, thus affecting the position and width of flexural wave bandgaps. To analyze the adjustment effect of the geometric parameters of the lightweight sandwich plate on the flexural wave bandgap, this section used the control variable method to study the influence of lattice constant a, thickness of the upper and lower panels e, thickness of the grid wall b, and core height of the lightweight sandwich plate H. The results are shown in Fig. 10.

It can be seen from Fig. 10(a) that as the lattice constant increases, the starting frequency and cutoff frequency of the flexural wave bandgap move to the low frequency, and the bandgap width of flexural wave also decreases. It can be seen from Fig. 10(b) that as the panel thickness increases, the upper and lower limits of the flexural wave bandgap move to the high frequency, and the upper limit of the bandgap rises faster than the lower limit, so the bandgap width also increases. The reason is that increasing

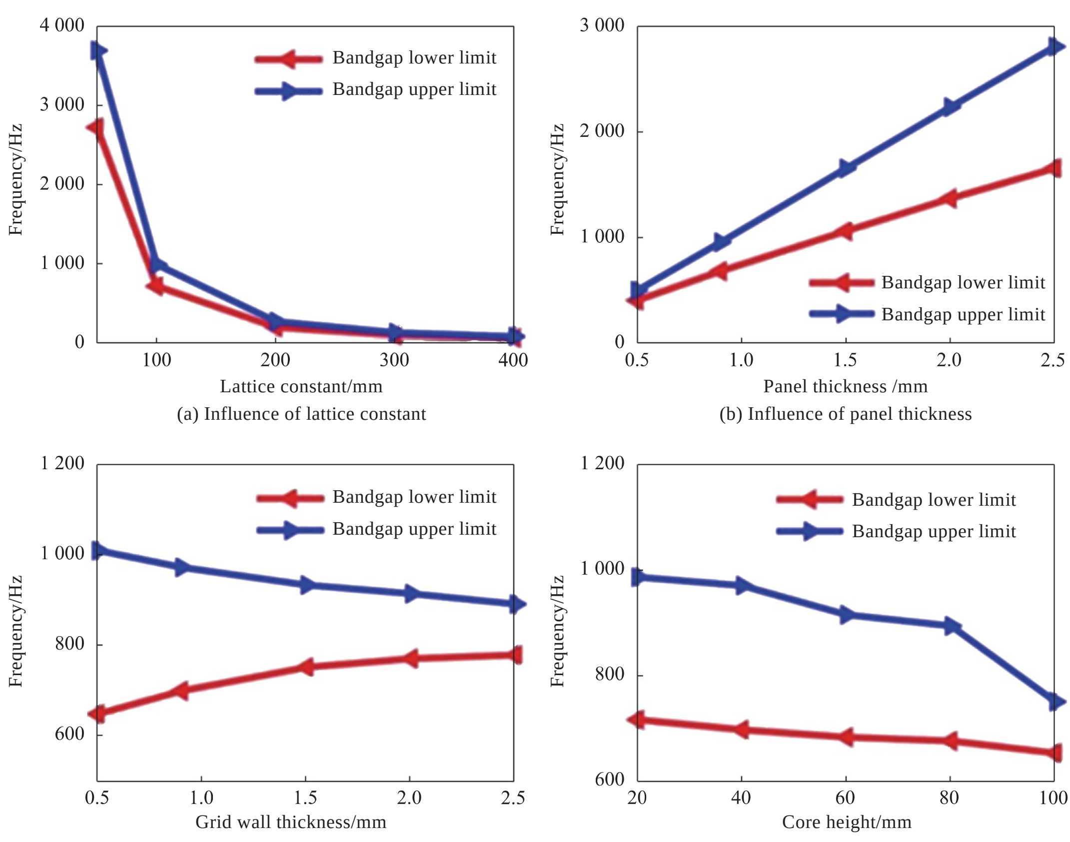

Fig. 10 Effects of geometric parameters on the flexural wave bandgap

the panel thickness will increase the overall bending stiffness of the sandwich plate, as well as the modal frequency of the asymmetric Lamb wave in the lightweight sandwich plate, thereby increasing the frequency range corresponding to the flexural wave bandgap. It can be seen from Fig. 10(c) that as the grid wall thickness increases, the lower limit of the flexural wave bandgap gradually increases while its upper limit gradually decreases, resulting in a decrease in the bandgap width. The reason is that increasing the grid wall thickness will increase the overall bending stiffness of the lightweight sandwich plate so that the starting frequency corresponding to the lower limit of the bandgap gradually increases. The grid core layer can be regarded as a connecting spring that transmits vibration between the upper and lower panels, so increasing the grid wall thickness will decrease the elasticity of the connecting spring and weaken the coupling effect between the upper and lower panels of the periodic lightweight sandwich plate, thereby decreasing the cutoff frequency corresponding to the upper limit of the bandgap. It can be seen from Fig. 10(d) that with the increase of the core height, the upper and lower limits of the bandgap move to the low frequency, and the bandgap width decreases as a whole. Due to the increase in the core height, the connection between the upper and lower panels of the lightweight sandwich plate is weakened, and the overall bending stiffness of the structure will decrease. Therefore, the starting frequency corresponding to the lower limit of the bandgap will move to the low frequency.

Based on the above parameter analysis, according to the generation mechanism of ship vibration and noise, active design and manual modulation on the frequency range for the flexural wave bandgap of the lightweight sandwich plate can be realized by adjusting the geometric parameters.

4 Conclusions

In this paper, the equivalent design of ship sandwich plates was carried out according to the principle of similarity theory. Based on the bandgap theory of phononic crystal and Bloch theorem, their numerical simulation model of wave propagation characteristics was established. By calculating the energy band structures and analyzing the transmission characteristics and primitive cell intrinsic displacement field, their flexural wave bandgaps and vibration and noise reduction characteristics were studied. The experiment on their vibration transmission and attenuation characteristics was carried out, and the influence of geometric parameters on the flexural wave bandgaps was analyzed. The following results are obtained:

1) Periodic sandwich plates of ships show flexural wave bandgaps and vibration attenuation in the high-frequency range of 699−971 Hz. There is a good sound insulation effect in the frequency range of the flexural wave bandgap, which can break through the limitation of the sound insulation mass law to a certain extent. Their bandgap generation mechanisms is mainly that the incident flexural wave is reflected back and forth at each periodic interface under the modulation of Bragg scattering and the flexural vibration mode disappears due to the destructive interference between the forward wave and the reverse wave. The experimental results verify their flexural wave bandgap and vibration reduction characteristics.

2) The structural parameters have a significant adjustment effect on the flexural wave bandgap. The increase in the equivalent elasticity of the core layer and the decrease in the overall stiffness are beneficial to the flexural wave bandgap moving to the low frequency. According to the generation mechanism of ship vibration and noise, the active design and artificial modulation on the frequency range of the flexural wave bandgap can be realized by adjusting geometric parameters, which provides a new technical way for vibration and noise reduction and acoustic stealth of ships.

References

[1] LIN T R, PAN J, O'SHEA P J, et al. A study of vibration and vibration control of ship structures [J]. Marine Structures, 2009, 22 (4): 730−743.

[2] KANDASAMY R, CUI F S, TOWNSEND N, et al. A review of vibration control methods for marine offshore structures [J]. Ocean Engineering, 2016, 127: 279−297.

[3] ZHANG B L, HAN Q L, ZHANG X M. Recent advances in vibration control of offshore platforms [J]. Nonlinear Dynamics, 2017, 89 (2): 755−771.

[4] WU C J, LEI Z Y, XU X T, et al. An analysis of low frequency propeller vibration and sound radiation characteristics: The Jellyfish effect [J]. Chinese Journal of Ship Research, 2020, 15 (5): 154−160 (in Chinese).

[5] YOU J Y, ZHAO Y, ZHANG G B, et al. Antiresonance vibration isolation analysis of shafting longitudinal vibration under elastic coupling of hull [J]. Chinese Journal of Ship Research, 2020, 15 (6): 137−142 (in Chinese).

[6] ZHAO X H, LI Y Y, YUAN Y C, et al. Study of Lex-tension type ship vibration isolation pedestal based on impedance mismatch principle [J]. Chinese Journal of Ship Research, 2021, 16 (3): 144−151 (in Chinese).

[7] LI Y G, ZHU L, CHEN T N. Plate-type elastic metamaterials for low-frequency broadband elastic wave attenuation [J]. Ultrasonics, 2017, 73: 34−42.

[8] HSU F C, LEE C I, HSU J C, et al. Acoustic band gaps in phononic crystal strip waveguides [J]. Applied Physics Letters, 2010, 96 (5): 051902.

[9] LI Y G, ZHOU L, ZHU L, et al. Flexural vibration band gap characteristics of ship plates with periodic vibration blocking masses [J]. Journal of Ship Mechanics, 2019, 23 (11): 1369−1375 (in Chinese).

[10] SUN Y G, LI S. Vibration band gap research of periodic stiffened plates [J]. Journal of Ship Mechanics, 2016, 20 (2): 142−147 (in Chinese).

[11] LI Y G, ZHOU Q W, ZHOU L, et al. Flexural wave band gaps and vibration attenuation characteristics in periodic bi-directionally orthogonal stiffened plates [J]. Ocean Engineering, 2019, 178: 95−103.

[12] RUAN Y D, LIANG X, HUA X Y, et al. Isolating low-frequency vibration from power systems on a ship using spiral phononic crystals [J]. Ocean Engineering, 2021, 225: 108804.

[13] GUO X, CUI H Y, HONG M. Research on vibration and noise reduction of local resonant phononic crystal plate [J]. Journal of Ship Mechanics, 2021, 25 (4): 509−516 (in Chinese).

[14] JIANG C J, XIANG Y, HE P, et al. Vibration attenuation behaviors of finite sandwich plates with periodic core [J]. Applied Acoustics, 2020, 157: 107009.

[15] CHEN J S, SHARMA B, SUN C T. Dynamic behaviour of sandwich structure containing spring-mass resonators [J]. Composite Structures, 2011, 93 (8): 2120−2125.

[16] CHEN J S, SUN C T. Reducing vibration of sandwich structures using antiresonance frequencies [J]. Composite Structures, 2012, 94 (9): 2819−2826.

[17] CHEN J S, SUN C T. Wave propagation in sandwich structures with resonators and periodic cores [J]. Journal of Sandwich Structures & Materials, 2013, 15 (3): 359−374.

[18] LI J Q, FAN X L, LI F M. Numerical and experimental study of a sandwich-like metamaterial plate for vibration suppression [J]. Composite Structures, 2020, 238: 111969.

[19] SONG Y B, FENG L P, WEN J H, et al. Reduction of the sound transmission of a periodic sandwich plate using the stop band concept [J]. Composite Structures, 2015, 128: 428−436.

[20] SONG Y B, FENG L P, LIU Z B, et al. Suppression of the vibration and sound radiation of a sandwich plate via periodic design [J]. International Journal of Mechanical Sciences, 2019, 150: 744−754.

[21] SONG Y B, WEN J H, TIAN H, et al. Vibration and sound properties of metamaterial sandwich panels with periodically attached resonators: Simulation and experiment study [J]. Journal of Sound and Vibration, 2020, 489: 115644.

[22] WANG X P, CHEN Y Y, ZHOU G J, et al. Synergetic coupling large-scale plate-type acoustic metamaterial panel for broadband sound insulation [J]. Journal of Sound and Vibration, 2019, 459: 114867.

[23] MA F Y, XU Y C, WU J H. Modal displacement method for extracting the bending wave bandgap of platetype acoustic metamaterials [J]. Applied Physics Express, 2019, 12 (7): 074004.

周期性舰船夹芯板弯曲波带隙与减振降噪研究

訾欢[1,2],李应刚[1,2,3],胡蜜[1,2],朱凤娜*[1,2],朱凌[1,2,3]

1 武汉理工大学 高性能舰船技术教育部重点实验室,湖北 武汉 430063

2 武汉理工大学 船海与能源动力工程学院,湖北 武汉 430063

3 武汉理工大学 三亚科教创新园,海南 三亚 572025

摘　要:[**目的**]旨在研究轻质夹芯板弹性波的传播规律与减振降噪机理。[**方法**]采用有限元方法结合布洛赫定理,对周期性夹芯板色散关系与弯曲波带隙特性进行研究,分析振动传输特性和声传输特性,研究轻质夹芯板减振降噪特性,并对轻质夹芯板振动传递衰减特性进行实验验证。[**结果**]研究结果表明,由于布拉格(Bragg)散射调制作用,轻质夹芯板在特定频段存在弯曲波带隙,弯曲振动带隙频率范围内具有良好的减振降噪效果。[**结论**]轻质夹芯板结构参数对弯曲波带隙具有显著的调节作用,为舰船结构振动噪声控制与声隐身设计提供了新的技术途径。

关键词: 周期性夹芯板; 弯曲波带隙; 布拉格散射; 减振降噪